Front. Earth Sci. 2023, 17(1): 4–17
https://doi.org/10.1007/s11707-022-0970-9

RESEARCH ARTICLE

Stress sensitivity of coal reservoir and its impact on coalbed methane production in the southern Qinshui Basin, north China

Huimin JIA[1], Yidong CAI (✉)[2], Qiujia HU[1], Cong ZHANG[1], Feng QIU[2], Bin FAN[1], Chonghao MAO[1]

1 CBM Exploration and Development Branch, PetroChina Huabei Oilfeld Company, Changzhi 046000, China
2 School of Energy Resources, China University of Geosciences, Beijing 100083, China

Abstract Stress sensitivity has significant negative effects on the permeability and production of coalbed methane (CBM) reservoirs. To effectively minimize these negative effects, the degree of stress sensitivity during the CBM production process should be carefully studied. In this work, the curvature of the stress-sensitivity curve was adopted to explore the degree of stress sensitivity, dividing the stress-sensitivity curve and the drainage process into five stress stages: sharp decrease, rapid decrease, low-speed decrease, slower decrease and harmless with four critical stress points—transition, sensitivity, relief and harmless. The actual stages were determined by the initial permeability, stress-sensitivity coefficient and difference between the reservoir pressure and desorption pressure. The four critical stress points did not completely exist in the stress-sensitivity curve. With an increase in the initial permeability of coal, the number of existing critical stresses increases, leading to different gas-water drainage strategies for CBM wells. For reservoirs with a certain stress-sensitivity coefficient, the permeability at the sensitive stress point was successively greater than that at the transition, relief and the harmless stresses. When the stress-sensitivity coefficient is different, the stage is different at the beginning of drainage, and with an increase in the stress-sensitivity coefficient, the decrease rate of the permeability increases. Therefore, the stress-sensitivity coefficient determines the ability to maintain stable CBM production. For well-fractured CBM reservoirs, with a high stress-sensitivity coefficient, permeability damage mainly occurs when the reservoir pressure is less than the relief stress; therefore, the depressurization rate should be slow. For CBM reservoirs with fewer natural fractures, the reverse applies, and the depressurization rate can be much faster. The higher the difference between the reservoir and desorption pressures, the higher the effective stress and permeability damage after desorption, resulting in a much longer drainage time and many difficulties for the desorption of coalbed methane. The findings of this study can help better understand and minimize the negative effects of stress sensitivity during the CBM production process.

Keywords coalbed methane, stress sensitivity, curvature, stages division, drainage

1 Introduction

Coalbed methane (CBM) exploitation or carbon capture and storage in coal seams would be important ways to achieve carbon neutrality (Zou et al., 2021). Three commercial CBM projects have been established in China such as the southern Qinshui Basin, eastern Ordos Basin, and southern Junggar Basin (Wang et al., 2021). A relatively long period of dewatering process exists before CBM exploitation due to unsaturated CBM reservoirs in China (Clarkson and Qanbari, 2016; Shi et al., 2019; Omotilewa et al., 2021). After the reservoir pressure drops below the critical desorption pressure through continuous pumping water, the CBM migrates and outputs through three linked stages: desorption, diffusion, and seepage (Ni et al., 2021; Liu et al., 2022). The permeability is an essential factor that determines the water drainage quantity and the production of CBM (Han et al., 2016; Kong et al., 2017; Wang et al., 2019). High-rank coal develops complex pore-fracture structure (Su et al., 2001; Cai et al., 2014; Busse et al., 2017; Fu et al., 2018; Zhang et al., 2019b; Liu et al., 2020; Liu et al., 2021), such as face and butt cleats, micro-fractures and matrix pores, resulting in strong stress sensitivity (Meng and Li, 2013; Meng et al., 2015; Li et al., 2017; Cheng

Received November 4, 2021; accepted January 17, 2022

E-mail: yidong.cai@cugb.edu.cn

et al., 2021). The stress sensitivity mainly depends on effective stress as well as the mechanical properties of coal. The stress sensitivity coefficient of coal permeability is inversely proportional to Young's modulus and porosity (Yan et al., 2019). With the increase of the effective stress, the elastic-plastic deformation leads to a sharp decrease of permeability at the beginning and then the decrease of which slows down (Li et al., 2021). The mechanical properties of organic component and the minerals in coal are greatly different (Li et al., 2021), so the coal matrix compressibility also effected by minerals, and its appearance, as well as coal rank and pore structure (Cai et al., 2018).

The attention to the influence of stress sensitivity has been paid during the process of drainage and production because of possible productivity damage caused in CBM wells (McKee et al., 1988; Tao et al., 2012; Li et al., 2014b; Li et al., 2019; Zhang et al., 2019c). The effective stress keeps increasing in the process of drainage as the reservoir pressure decreases and the overburden pressure is constant (Zhang et al., 2010; Huang et al., 2019; Wang et al., 2021). And also, the reservoir permeability continues to decline before the matrix shrinkage dominates the change of permeability (Palmer and Mansoori, 1998; Guo et al., 2014; St. George and Barakat, 2001; Geng et al., 2017; Zhu et al., 2018). Therefore, the stress sensitivity of coal seam determines the drainage efficiency and the dropping scope of reservoir pressure (Hou et al., 2015; Xu et al., 2017). Meanwhile, minimizing the damage of permeability in coal seams is key to achieve efficient production and development of CBM (Feng et al., 2018; Zhang et al., 2019d). The curves of stress sensitivity are commonly used for the characterization of the its degree (Guo et al., 2014; Zhang et al., 2018; Feng et al., 2019; Zhang et al., 2019a; Tang et al., 2021). With much more attention to the decrease of the permeability, most researches ignore the change of the stress sensitivity degree during the increase of the effective stress (McKee et al., 1988; Palmer and Mansoori, 1998; Jia et al., 2017; Zhao et al., 2018; Tang et al., 2021), and regards the stress sensitivity as a constant or the average value of a certain reservoir.

Three parameters—the stress-sensitivity coefficient, permeability modulus, and the permeability damage rate—are usually applied to evaluate the degree of stress sensitivity (Chen et al., 2012; Li et al., 2014a). The stress-sensitivity coefficient, a constant, is convenient for the comparison of different coal samples but cannot, exactly reflect the change of stress sensitivity exactly as the effective stress increases (Liu et al., 2018a). The permeability modulus and permeability damage coefficient reveal a constant change in the stress sensitivity with an increase in the effective stress. However, the permeability modulus is only an essential concept (Xiao et al., 2021), whereas the permeability damage rate with much clearer physical meanings can be calculated by the negative of the first derivative of permeability versus stress. Despite the large number of studies on stress sensitivity, few have focused on the different stages of stress sensitivity for the same reservoir during different effective stress stages. In this work, the curvature of the stress-sensitivity curve was adopted to explore the degree of stress sensitivity and divide the stress-sensitivity curve as well as the drainage process a coalbed methane (CBM) well into five stages. Although the stress-sensitivity curves of Chengzhuang, Zhengzhuang and Hancheng coal have been analyzed based on the curvature analysis method (Chen et al., 2014), the analysis of the stress sensitivity for different drainage stages and the effects on the drainage strategies are still absent. Furthermore, this work also studied the factors affecting the stage division of the stress-sensitivity curve and provided appropriate drainage strategies.

This work was carried out in the following steps. First, the experimental section was set up, and stress sensitivity experiments were carried out using samples from the Fanzhuang–Zhengzhuang Block and the Qinnandong Blocks. Second, the experimental results were analyzed, a mathematical model of stress-sensitivity curves was proposed based on curve fitting, and the mathematical model was derived theoretically. Then, the curvature of the stress-sensitivity curve was adopted to explore the degree of stress sensitivity by dividing the process into five stages, and the factors affecting the stage divisions were analyzed. Finally, appropriate drainage strategies were proposed.

2 Stress sensitivity experiment of coal samples

2.1 Coal sampling and basic coal information

Samples were taken from coal cores of CBM wells in the Fanzhuang–Zhengzhuang Block and Qinnandong Block of the southern Qinshui Basin (Fig. 1), and nine samples were selected to conduct stress-sensitivity experiments. Samples 1–4 come from the Fanzhuang–Zhengzhuagn Block and Samples 5–9 come from the Qinnandong Block. The basic parameters of the coal samples are presented in Table 1.

2.2 Experimental conditions and procedures

Cylindrical coal core samples with a diameter of 50 mm and length of 100 mm were dried at 105°C until the weight was constant. The experimental temperature was 20°C, and the helium was used as the injection gas. During the experiments, a constant pressure was used to inject the helium, and the confining pressure was changed to simulate different effective stress conditions. The maximum value of the effective stress in the experiments was set as 6.5 MPa for the Fanzhuang–Zhengzhuang

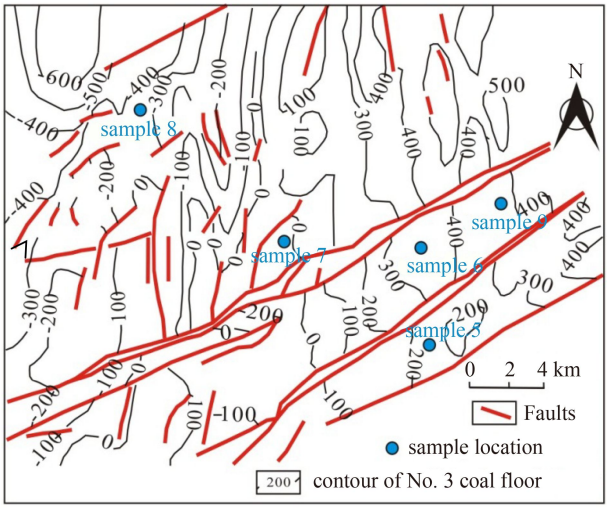

(a) Qinnandong Block

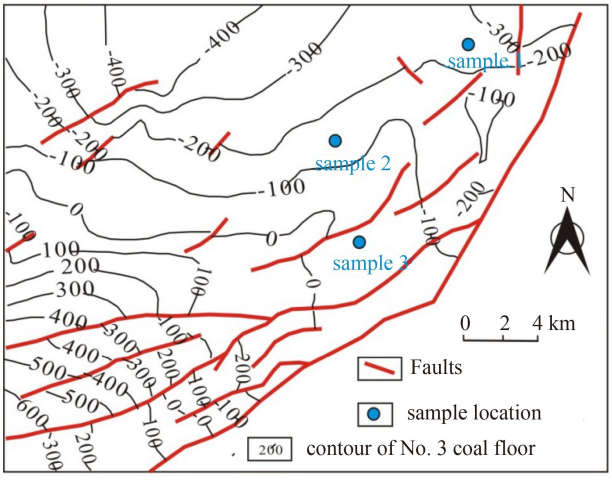

(b) Zhengzhuang Block

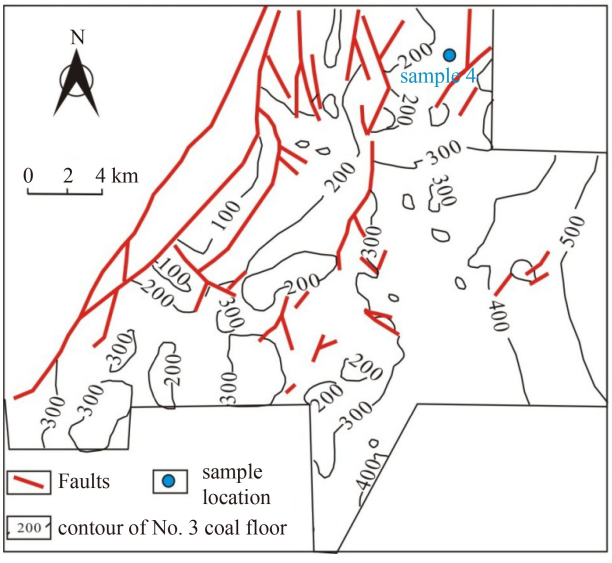

(c) Fanzhuang Block

Fig. 1 Sample spots in Fanzhuang–Zhengzhuang and Qinnandong Block.

Block samples, and 9 MPa for the Qinnandong Block samples, according to the actual average original reservoir pressure. Because the overburden pressure was constant and the reservoir pressure exhibited a decreasing trend during CBM production, the effective stress increases as the reservoir pressure decreased. The experimental procedures were performed in accordance with the Chinese Standard SY/T 5358-2010, and the results are shown in Fig. 2.

2.3 Experimental results

The relation between effective stress versus permeability presented a decrease exponential function, as shown in Fig. 2. Although the coals were different, the results had similar performance, which also the same as the results of the previous experiments by coals from other blocks (Jasinge et al., 2011; Li et al., 2013; Fan and Liu, 2019).

The exponential function expression was as (Zhang et al., 2015; Jia et al., 2017; Zhao et al., 2018; Lin et al., 2020; Zhou et al., 2020)

$$k = k_0 e^{-C\sigma_e}, \tag{1}$$

where k_0 is the initial permeability, mD, that is, the permeability when σ_e is 0 MPa; σ_e is the effective stress, MPa; k is the permeability under different effective stresses, mD; C is the stress sensitivity coefficient, MPa^{-1}. The stress-sensitivity coefficient of coal seam represents the degree of the stress sensitivity. The greater the coefficient, the stronger the stress sensitivity.

As shown in Table 2, the stress-sensitivity coefficient of coals from different CBM blocks in China ranged from 0.1 to 1.5 MPa^{-1}, and the stress-sensitivity coefficient of coals with no obvious fractures was all lower than 0.5 MPa^{-1}. The stress-sensitivity coefficient of the coals with well-developed fractures was relatively high, and the maximum value is up to 1.5 MPa^{-1}.

3 Theoretical derivation of mathematical model of stress sensitivity for coal reservoir

Equation (1) is an empirical equation, which also can be derived mathematically. The permeability of the matrix is extremely low; therefore, the permeability of coal mainly depends on the permeability of cleats. By simplifying the cleat system of coal into a bundle of matchstick, and the calculation formula of the fracture permeability of coal can be expressed as (Reiss, 1980)

$$k_f = \frac{1}{48} a^2 \varphi_f^3, \tag{2}$$

where k_f is the fracture permeability, mD; a is the fracture width, cm; φ_f is the fracture porosity.

Based on the bundled conceptual matchstick model and

Table 1 Basic parameters of the selected nine coal samples from southern Qinshui Basin

Sample ID	Permeability/ mD	Proximate analysis/%				Maceral content/%		$R_{o,max}$ /%
		M_{ad}	A_{ad}	V_{ad}	FC_{ad}	Vitrinite	Inertinite	
Sample 1	0.075	1.22	11.55	7.66	79.57	70.10	29.90	3.32
Sample 2	2.900	1.87	14.32	7.96	75.85	80.10	19.90	3.25
Sample 3	0.640	1.15	12.36	7.17	79.32	72.10	27.90	3.27
Sample 4	2.200	1.09	18.1	8.47	72.34	62.20	37.80	3.32
Sample 5	0.170	0.90	14.78	12.39	71.93	70.80	29.20	2.24
Sample 6	0.161	0.89	10.65	11.10	77.36	75.40	24.60	2.39
Sample 7	0.870	0.89	11.16	10.17	77.78	69.60	30.40	2.51
Sample 8	0.173	0.83	12.14	10.09	76.94	77.90	22.10	2.57
Sample 9	0.211	0.7	13.83	11.83	73.64	66.60	33.40	2.20

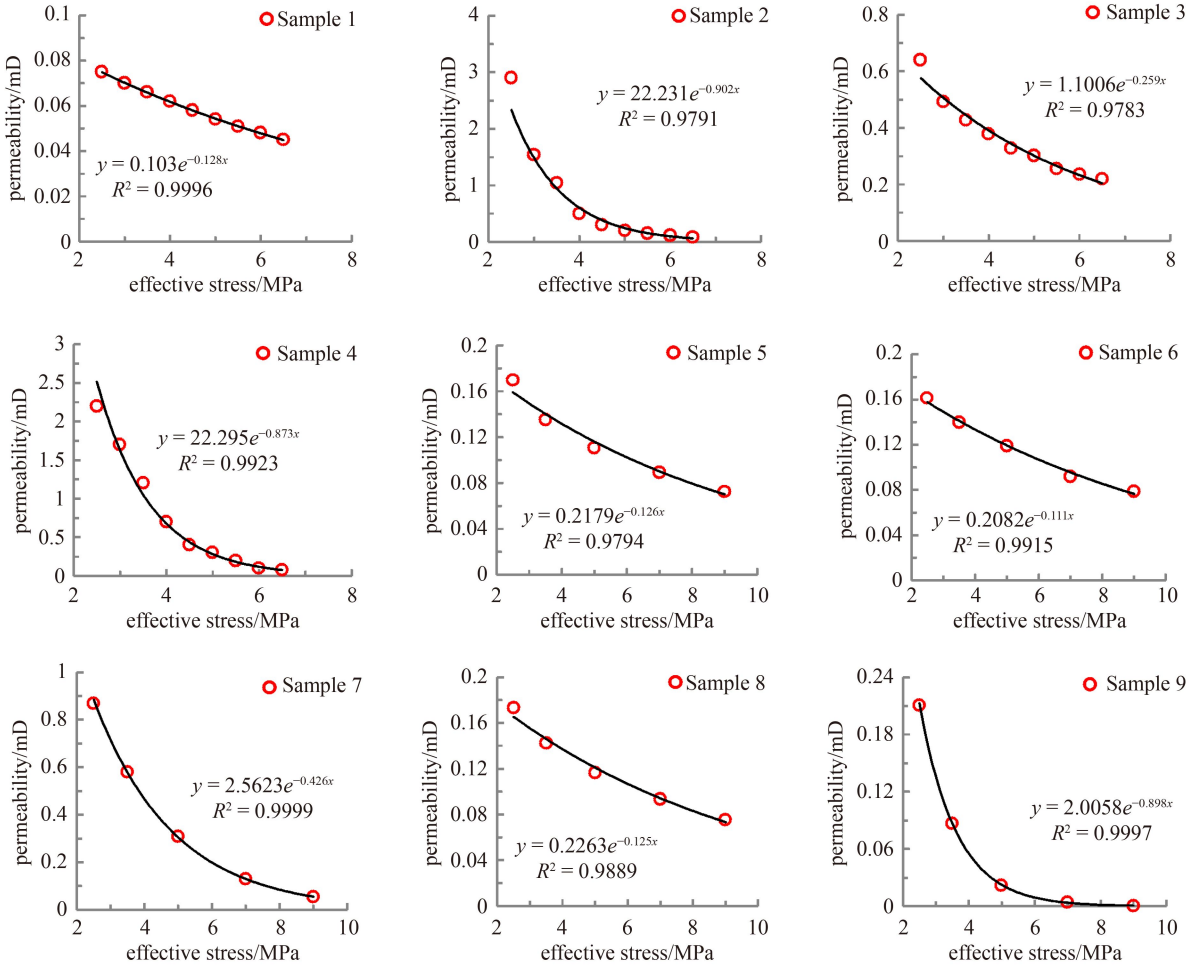

Fig. 2 The relationship between effective stress and permeability for selected 9 coals.

Eq. (2), the stress sensitivity mathematical model for fracture permeability was established (Seidle et al., 1992), which is

$$\frac{k_f}{k_{f0}} = e^{-3C_f(\sigma_e-\sigma_{e0})}, \tag{3}$$

where k_{f0} is the original fracture permeability, mD; C_f is the stress-sensitivity coefficient of fracture, MPa^{-1} for coals under geostress, the permeability of coal is approximately equal to the permeability of its fracture networks (Seidle et al., 1992; Chen et al., 2013; Jia et al., 2017), then Eq. (3) can be rewritten as Eq. (1).

Table 2 Distribution range of the stress-sensitivity coefficient for different CBM blocks in China

CBM blocks	Fracture development	Number of coal samples	The stress sensitivity coefficient/MPa^{-1}		References
			Value range	Average value	
Zhengzhuang Block in Qinshui Basin	WDNO [a)]	4	0.36–0.90	0.54	Zhang et al. (2010)
Fanzhuang–Zhengzhuang Block in Qinshui Basin	WDNO	9	0.11–0.90	0.30	This work
Qiannandong Block in Qinshui Basin	No obvious fractures	13	0.23–0.48	0.36	Zhao et al. (2018)
Southern Qinshui Basin	well developed	3	0.71–1.48	1.18	Jia et al. (2017)
Qinshui Basin	NA[b)]	8	0.11–0.26	0.2	Huang et al. (2019)
Pingdingshan Mine	NA	22	0.13–0.85	0.27	Zhang et al. (2019d)

Notes: [a)] WDNO: samples both with well-developed fractures and no obvious fractures; [b)] NA: not available.

4 Division of stress-sensitivity stages

4.1 Permeability damage rate

With an increase in the effective stress, the reservoir permeability decreased. The rate of permeability damage was used to characterize the degree of damage of the effective stress on the permeability, and was defined as the permeability reduction value versus the increase in the unit of effective stress; that is, the negative of the first derivative of k as

$$k_D = -k' = k_0 C e^{-C\sigma}, \tag{4}$$

where k_D is the permeability damage rate; k' is the first-derivative of k. Equation (4) indicates that the permeability damage rate decreases and the decrease rate becomes smaller, with the increase of the effective stress.

4.2 Curvature of stress-sensitivity curve

The large curvature of the stress-sensitivity curve (Meng et al., 2014) indicates a severe permeability damage rate for the same increase in the range of effective stress. The curvature calculation formula of stress-sensitivity curve is as follows:

$$K_q = \frac{|k''|}{(1+k'^2)^{3/2}} = \frac{C^2 k_0 e^{-C\sigma}}{(1+k_0{}^2 C^2 e^{-2C\sigma})^{3/2}}, \tag{5}$$

where k'' is the second derivative of k; K_q is the curvature of the stress-sensitive curve.

With an increase in the effective stress, the curvature of the stress-sensitivity curve, for Samples 2, 4, 7, and 9 increased up to the peak and then decreased quickly. This phenomenon illustrates that the permeability damage of these samples was initially high and then decreased drastically. The curvature for Samples 1, 3, 5, 6, and 8 kept decreasing, and the value of K_q was relatively low, which illustrates that the curvature curve of these samples was only part of the curve for the other samples, and the permeability damage was at a low level with an increase in the effective stress, as shown in Fig. 3.

4.3 Critical stress points

4.3.1 Transition stress

The transition stress, denoted as σ_z, was defined as the effective stress corresponding to the maximum curvature value (Fig. 4). When the value of the curvature reached its maximum, the decrease in the permeability damage rate slowed down with an increase in the effective stress. The transition stress is a cut-off point between the fast and slow decrease stages of the permeability damage rate. The transition stress can be calculated when the first derivative of the curvature curve is 0; that is

$$K_q' = \frac{k_0 C^3 e^{-C\sigma} \left(2k_0{}^2 C^2 e^{-2C\sigma} - 1\right)}{\left(1+k_0{}^3 C^2 e^{-2C\sigma}\right)^{\frac{5}{2}}} = 0, \tag{6}$$

where K_q' is the first derivative of the curvature. According to Eq. (6), the transition stress is calculated as

$$\sigma_z = \frac{\ln\left(\sqrt{2}k_D C\right)}{c}, \tag{7}$$

where σ_z is the transition stress, MPa. Therefore, the permeability damage rate at transition stress is a constant, $k_D = \frac{\sqrt{2}}{2}$ mD/MPa.

4.3.2 Sensitive stress and relief stress

The sensitive stress and relief stress can be derived as

$$K_q'' = \frac{10k_0{}^3 C^6 e^{-3C\sigma} - 4k_0{}^5 C^8 e^{-5C\sigma} - k_0 C^4 e^{-C\sigma}}{\left(1+k_0{}^2 C^2 e^{-2C\sigma}\right)^{\frac{7}{2}}} = 0, \tag{8}$$

where K_q'' is the second derivative of the curvature. The smaller solution to Eq. (8) is defined as the sensitive stress, and the larger solution is defined as the relief stress.

The sensitive stress is the cut-off point of the fast decrease stage, and is calculated as

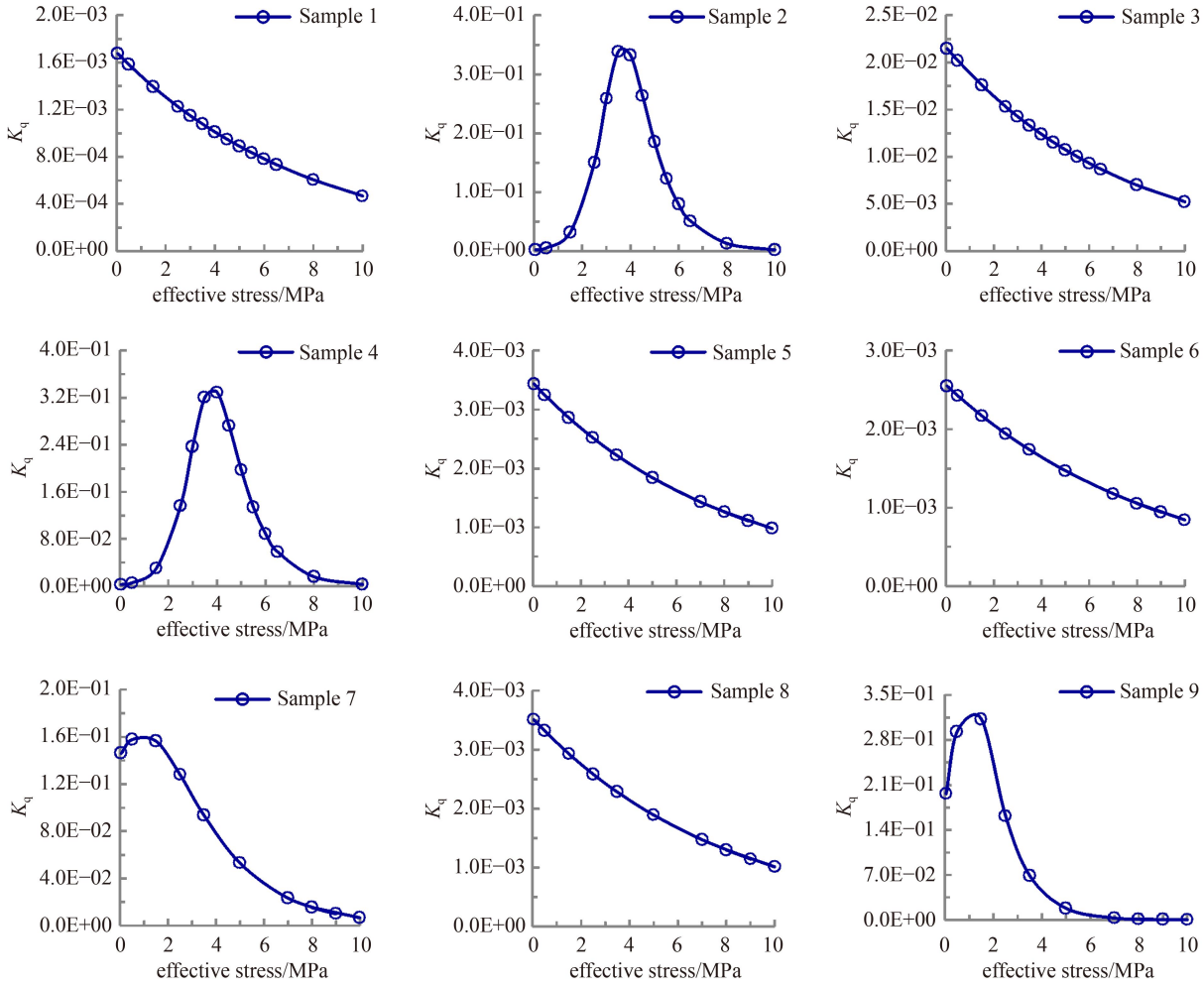

Fig. 3 Curvature of stress sensitivity curve versus effective stress of 9 coal samples.

$$\sigma_m = \frac{\ln\dfrac{2k_0C}{\sqrt{5+\sqrt{21}}}}{C}. \tag{9}$$

Relief stress is the cut-off point of the slow decrease stage, and is calculated as

$$\sigma_h = \frac{\ln\dfrac{2k_0C}{\sqrt{5-\sqrt{21}}}}{C}. \tag{10}$$

By substituting Eq. (9) and Eq. (10) into Eq. (4), the permeability damage rates at the sensitive and relief stresses were $\frac{\sqrt{5+\sqrt{21}}}{2}$ mD/MPa and $\frac{\sqrt{5-\sqrt{21}}}{2}$ mD/MPa, respectively. Figure 5 shows the second derivative of the stress sensitivity curvature for the nine coal samples. For Samples 1, 3, 5, 6, and 8, there were no sensitive and relief stress, while for Sample 7, there was only relief stress.

4.3.3 Harmless stress

Harmless stress occurs, when the permeability damage rate is 0.01 mD/MPa. When the stress was greater than the harmless stress, the damage to the permeability caused by the stress increase was negligible. The harmless stress can be calculated when $k_D = 0.01$, which is

$$\sigma_n = \frac{1}{C}\ln\frac{k_0C}{0.01}, \tag{11}$$

where σ_n is the harmless stress, MPa.

4.3.4 Stage division method

Based on the relationship between the effective stress and permeability and the regression of Sample 9 (Fig. 2), the extended curve for a larger effective stress is presented. Figure 6 shows that the sharp decrease stage ① was short, the ratio of permeability damage was low, the effective stress was smaller than the sensitive stress, and the permeability damage rate was larger than $\frac{\sqrt{5+\sqrt{21}}}{2}$

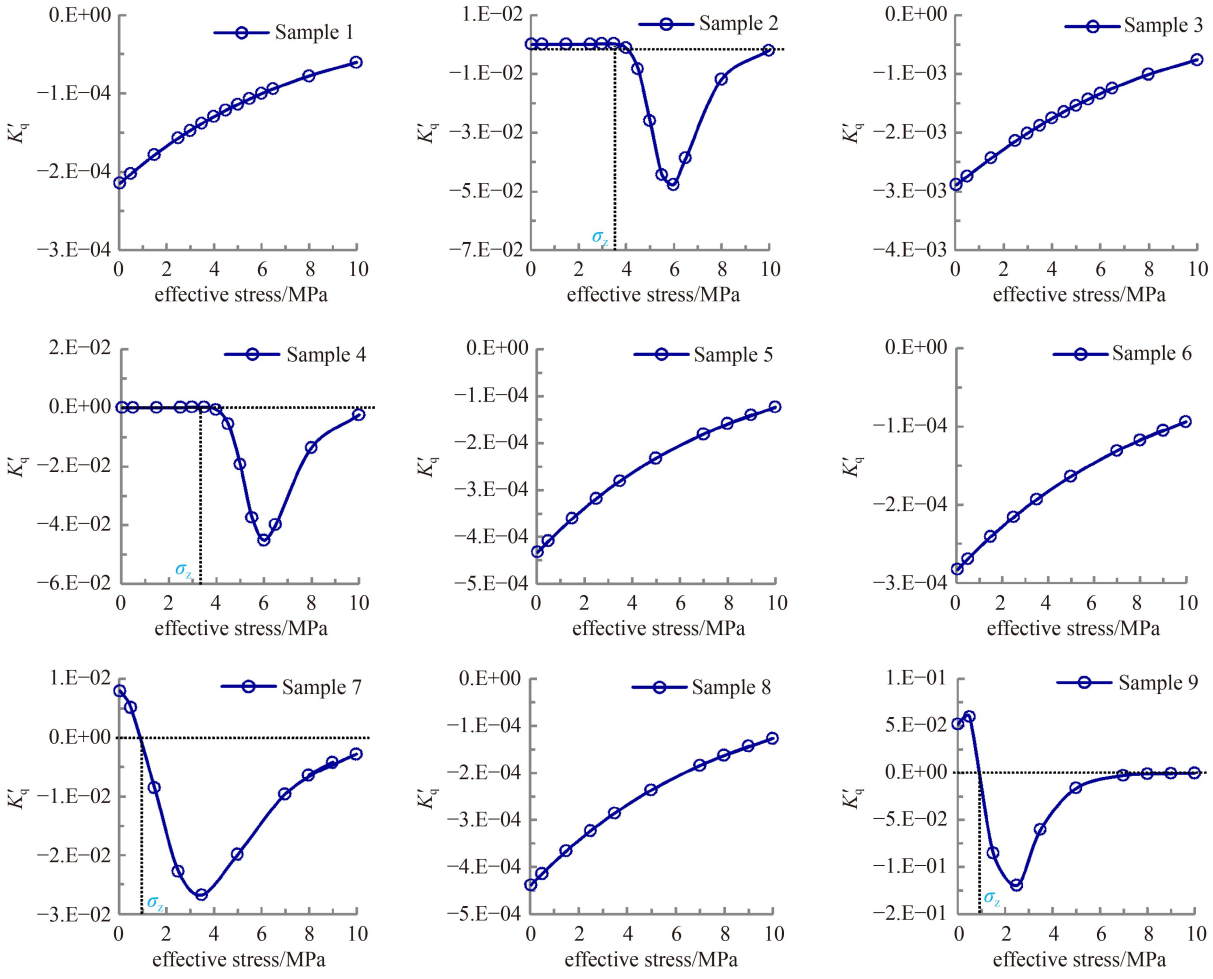

Fig. 4 The first derivative of stress sensitivity curvature.

mD/MPa. In the rapid decrease stage ②, the effective stress was between the sensitive stress and transition stress, and the permeability damage rate varied from $\frac{\sqrt{2}}{2}$ mD/MPa to $\frac{\sqrt{5+\sqrt{21}}}{2}$ mD/MPa. This is the main stage of permeability damage. In the low-speed decrease stage ③, the effective stress was between the transition and the relief stresses, and the permeability damage rate was in the range of $\frac{\sqrt{5-\sqrt{21}}}{2}$ mD/MPa and $\frac{\sqrt{2}}{2}$ mD/MPa. The permeability damage at this stage was still significant. In the slower decrease stage ④, the effective stress was between the relief and the harmless stresses, and the permeability damage rate changed from $\frac{\sqrt{5-\sqrt{21}}}{2}$ mD/MPa to 0.01 mD/MPa. The permeability damage at this stage was still significant. In the harmless stage ⑤, the effective stress was larger than that of the harmless stress, and the permeability damage rate was smaller than 0.01 mD/MPa, and the permeability damage was negligible.

The stress-sensitivity curves of Samples 2, 4, and 9 progressed through all of the above five stages with an increase in the effective stress. However, the stress sensitivity curves of Samples 1, 3, 5, 6, and 8 exhibited only two stages as the effective stress increased. And for Sample 7, the permeability experienced four stages without the sensitivity stress. To ensure the completeness of the stage division, all five stages were retained in this work, despite the difference in the actual stages of the stress-sensitivity curve for different coals owing to the difference in the initial permeability and stress-sensitivity coefficient. Although there were no obvious cut-off points on the stress versus permeability sensitivity curve (Figs. 2 and 6), it would take more than a year to lower the bottom-hole flow pressure from the reservoir pressure to the smallest value, with a daily depressurization rate of only 0.001–0.1 MPa. Therefore, it is necessary to accurately determine the cut-off points of permeability with an increase in effective stress based on the curvature of the stress-sensitivity curve.

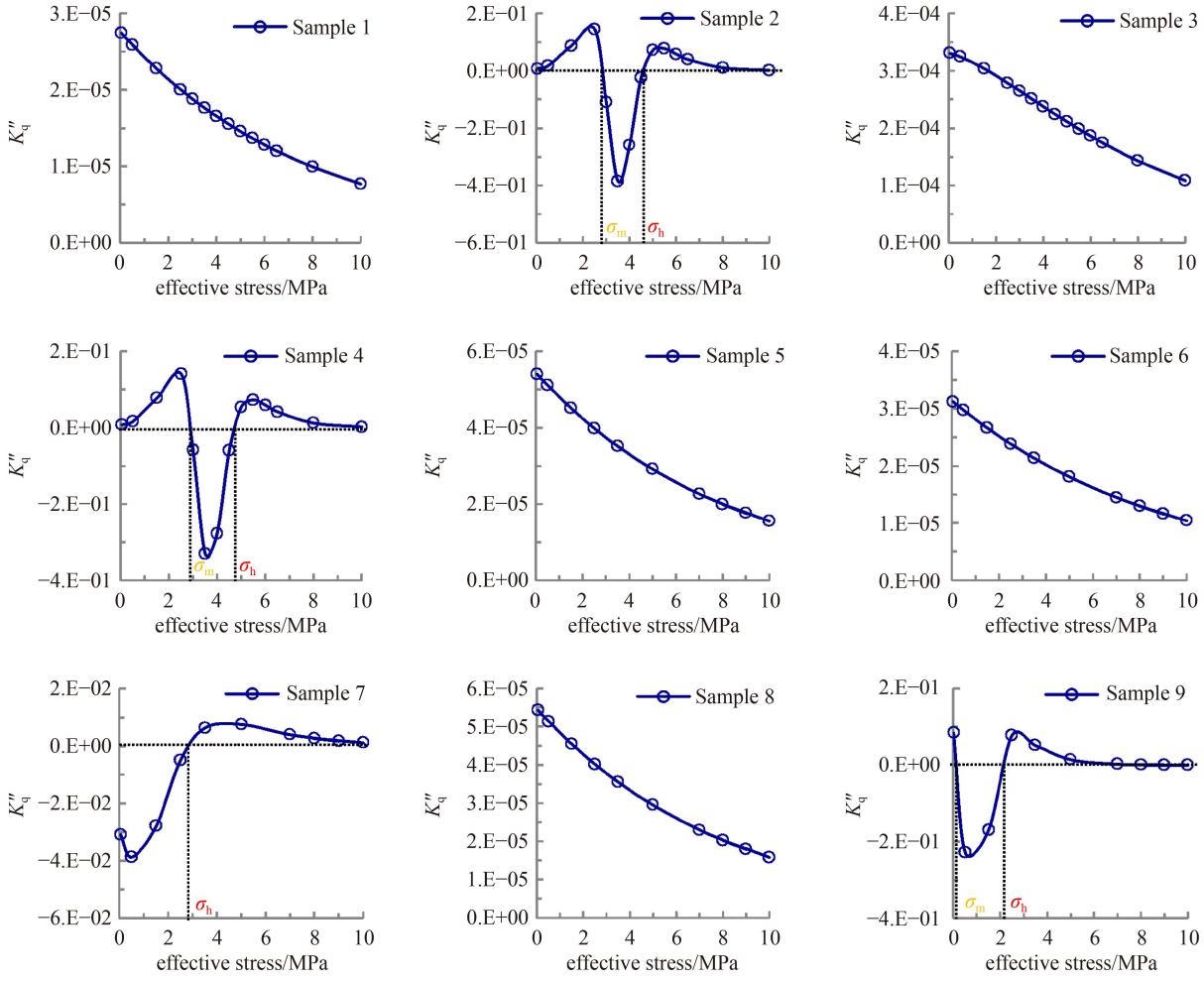

Fig. 5 The second derivative of stress-sensitivity curvature.

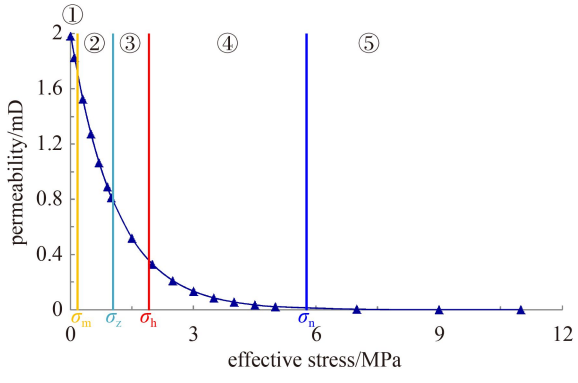

Fig. 6 Stages division of stress sensitivity curve of for sample 9.

5 Significance for CBM drainage

Continuous water drainage from CBM well causes the reservoir pressure to drop below the desorption pressure; thus, methane can be produced by the desorption and seepage processes (Ni et al., 2021; Liu et al., 2022). For an actual CBM reservoir, the reservoir pressure, effective stress, and overlying pressure are in equilibrium. During the drainage process, the effective stress increases as the reservoir pressure decreases (Zhang et al., 2010; Huang et al., 2019; Wang et al., 2021), indicating that the effective stress of a coal reservoir increases during CBM development.

5.1 Effects of initial permeability

A coal reservoir with a permeability less than 0.01 mD is tight (Sun et al., 2014). The permeability of coal reservoirs in China is generally between 0.01 mD and 10 mD, and most reservoirs have permeability lower than 1 mD. To analyze the effects of initial permeability on stress sensitivity without the interference of the stress-sensitivity coefficient, three stress-sensitivity curves with initial permeabilities of 1 mD, 0.5 mD, and 0.05 mD and a constant stress-sensitivity coefficient of 0.902 MPa^{-1} were used, based on Sample 2, by changing only the initial permeability as shown in Fig. 7. The curves with initial permeabilities of 1 mD, 0.5 mD, and 0.05 mD represent the stress-sensitivity characteristics of high, medium, and low permeability reservoirs, respectively. According to the stage division method, the three stress-

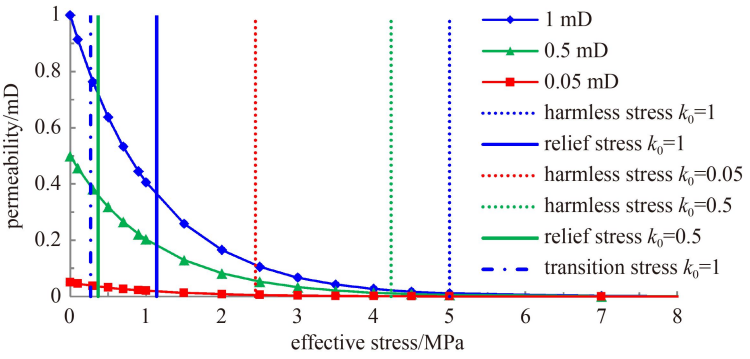

Fig. 7 Effect of initial permeability of coal on stage division of stress-sensitivity curve of Sample 2.

sensitivity curves were divided into different stages showing that four critical stress points partially existed in these curves. When the permeability was 0.05 mD, the stress-sensitivity curves even had only one critical stress point. With an increase in the initial reservoir permeability, the number of critical stress points of the coal reservoir gradually increased. When the permeability was 0.5 mD, the values of the sensitive and transition stresses were negative. There were only two critical stress points—the relief stress and harmless stress—and the stress-sensitivity curve was divided into three stages. When the permeability was 1 mD, there were three critical stress points: transition stress, relief stress, and harmless stress. The stress-sensitivity curve was divided into four stages: rapid decrease, low-speed decrease, slower decrease and harmless.

In the rapid decrease stage, although the permeability damage rate caused by the increase in effective stress was high, the absolute permeability was still high. The depressurization rate of the bottom-hole flow pressure of a CBM well should be relatively fast (0.05–0.07 MPa/d) to improve the depressurization efficiency. In the low-speed decrease stage, the depressurization rate should be set at a relatively slow rate (0.03 MPa/d) to protect the reservoir permeability and extend the depressurization and desorption ranges. In the slower decrease stage, the depressurization rate should be lowered at a relatively fast rate of 0.03–0.05 MPa/d to enhance the production pressure difference and improve the efficiency of water drainage. In the harmless stage, the permeability damage is very low; therefore, the depressurization rate has little effect on permeability.

The production curve for the medium-permeability reservoir in Fig. 8(a) shows that when the bottom-hole flow pressure was greater than 5.1 MPa, the depressurization rate was controlled to 0.05 MPa/d. When

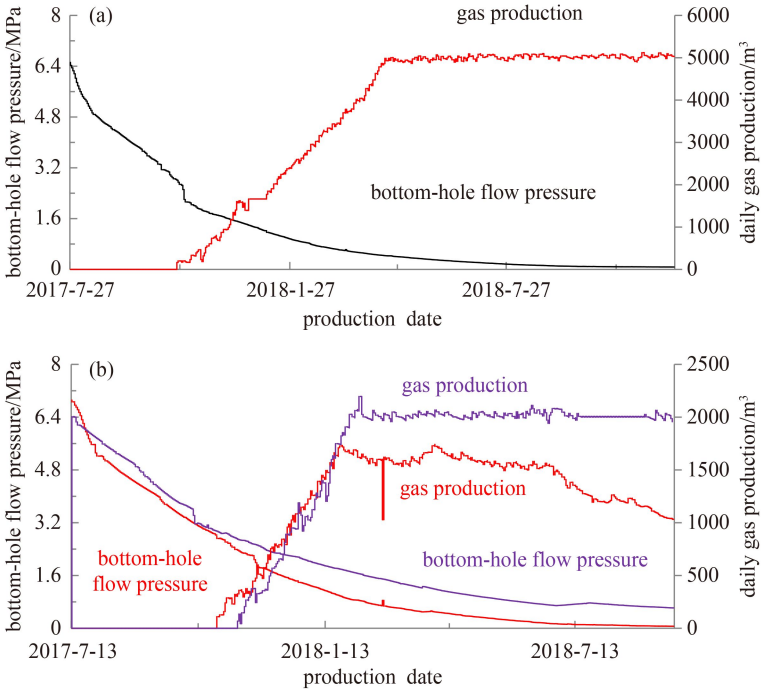

Fig. 8 The effect of the depressurization rate on the production of wells with different initial permeability. (a) Production curve for medium-permeability reservoir; (b) Production curve for low-permeability reservoir.

the bottom-hole flow pressure decreased from 3.0 MPa to 5.1 MPa, the depressurization rate became 0.03 MPa/d; when the bottom-hole flow pressure was reduced from 3.0 MPa to 1.2 MPa, the depressurization rate was controlled between 0.03 MPa/d and 0.05 MPa/d, resulting in a daily gas production of 5000 m^3/d that fully released CBM productivity. For low-permeability wells, with a relatively lower depressurization rate, the daily gas production was higher with a long stable production time (Fig. 8(b)).

5.2 Effect of stress-sensitivity coefficient

The initial permeability at different critical stress points vs. the stress-sensitivity coefficients in Fig. 9(a) shows that for formations with a certain stress-sensitivity coefficient, the permeability at sensitive stress was successively greater than that at the transition, relief and harmless stresses. For a coal reservoir with a determined stress-sensitivity coefficient, the actual initial permeability was higher than that shown in Fig. 9(a). When critical stress points existed in the stress-sensitivity curve, the permeability at the critical stress points were the minimum values as shown in Fig. 9(a). Comparing the minimum permeability, the larger the stress-sensitivity coefficients, the smaller the minimum permeability at the critical stress points (Fig. 9(a)).

The stress-sensitivity coefficients varied for CBM reservoirs with different pore and fracture structures (Bussea et al., 2017; Geng et al., 2017; Li et al., 2020; Cheng et al., 2021). The stress-sensitivity coefficient is larger when the fractures are well developed (Jia et al., 2017). The stress-sensitivity curve of Sample 3 with a stress-sensitivity coefficient of 0.26 MPa^{-1} (Fig. 2) indicates that the natural fractures were less developed. To analyze the effects of stress-sensitivity coefficient on the stage division, a comparative stress-sensitivity curve was established based on the stress-sensitivity curve of Sample 3 by changing only the stress-sensitivity coefficient to 0.9 MPa^{-1} as shown in Fig. 9(b), which represents coal where natural fractures are well-developed. Even if a reservoir's initial permeability and pressure drop (effective stress) are the same, the dynamic permeability of the reservoir will still be different. A reservoir stress-sensitivity coefficient of 0.9 MPa^{-1} occurred during the rapid decrease stage, while a stress-sensitivity coefficient of 0.26 MPa^{-1} occurred during the slower decrease stage at the beginning of drainage as shown in Fig. 9. Therefore, at the beginning of drainage, the higher the stress-sensitivity coefficient, the faster rate of decrease in permeability. This causes a decrease in the drainage efficiency and gas production. Therefore, the unimodal type curve of gas and water production should be easy to form, which means that the stress-sensitivity coefficient determines the productivity, and the greater the stress-sensitivity coefficient is, the shorter the time

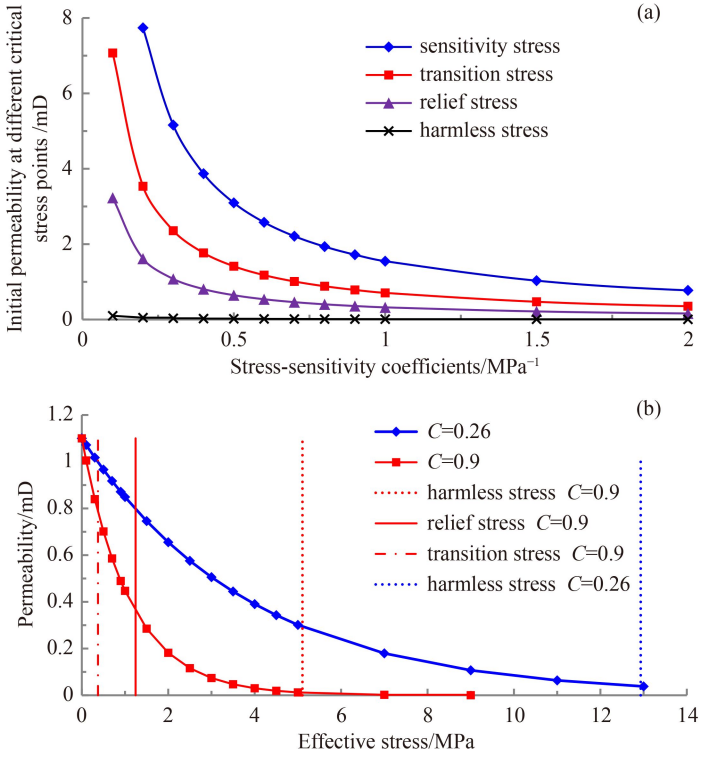

Fig. 9 Effect of stress-sensitivity coefficient on the division of the stress-sensitivity curve. (a) Minimum permeability at different critical stress points for different stress-sensitivity coefficients; (b) Effect of effective stress versus permeability on the division stage of stress-sensitivity curve.

keeping the production stable.

Figure 9(b) shows that when the stress-sensitivity coefficient was 0.9 MPa^{-1}, the permeability damage mainly occurred in the stage where the reservoir pressure was less than the relief stress, whereas when the stress-sensitivity coefficient was 0.26 MPa^{-1}, the calculated relief stress was negative. The permeability damage mainly occurred in the stage where the reservoir pressure was higher than the relief stress. Therefore, for reservoirs with well-developed natural fractures and strong stress sensitivity, the depressurization rate should be slow (generally 0.01–0.03 MPa/d); a reservoir pressure higher than the relief stress will be favorable for achieving the greatest amount of water drainage and the widest scope of pressure drop. For reservoirs with fewer natural fractures and poor stress sensitivity, when a reservoir pressure is higher than the relief stress, the pressure can be reduced quickly (generally 0.05–0.07 MPa/d) to expand the production pressure difference, improve the drainage efficiency, and shorten the time required to reach the designed production.

5.3 Effect of difference between reservoir and desorption pressures

The gas desorption rate of a CBM well is determined by reservoir permeability, reservoir pressure, and desorption pressure. When the initial permeability is constant, the difference between the reservoir and desorption pressures determines the difficulty of gas desorption (Sun et al., 2019), which reflects the difficulty of gas desorption more accurately than the ratio of the critical desorption pressure to the reservoir pressure (Ni et al., 2021). The larger the difference between the reservoir and desorption pressures, the greater the effective stress; therefore, the higher the dynamic permeability damage, and the longer the drainage time needed before desorption, the more difficult it is for the desorption of CBM. The smaller the difference between the reservoir pressure and desorption pressure, the smaller the damage to the reservoir dynamic permeability, and the more favorable the drainage and high gas production. Reservoirs with reservoir and desorption pressure differences larger than the harmless stress have an extremely low permeability after desorption (Fig. 9(a)), and lead to a short burst of gas production, even though the gas contents may be very high. This type of CBM normally has a high production rate by improving reservoir permeability through hydraulic stimulation (Su et al., 2018) or by decreasing the reservoir pressure (Liu et al., 2018b). For wells with relatively low gas contents, the dynamic permeability can still be very high after desorption if the difference between the reservoir and desorption pressures is smaller than the transition stress or the sensitive stress, which also results in a high drainage efficiency and high production rate.

6 Summary and Conclusions

The curvature of the stress-sensitivity curve was adopted to divide the curve into five stages based on four critical stress points. The effects of the initial permeability, stress-sensitivity coefficient, and the difference between reservoir and desorption pressures were also assessed, and appropriate drainage strategies were proposed. The following conclusions were drawn.

1) The greater the curvature, the greater the permeability damage rate. Four critical stress points—transition, sensitive, relief, and harmless—divides the stress-sensitivity curve into five stages: sharp decrease, rapid decrease, low-speed decrease, slower decrease, and harmless. The sharp decrease and rapid decrease stages were the main damage stages of permeability.

2) The four critical stress points do not completely exist in one stress-sensitivity curve. The higher the original permeability of a reservoir is, the more critical stress points exist. Drainage strategies should differ for reservoirs with different original permeabilities.

3) For reservoirs with certain stress-sensitivity coefficients, the permeability at sensitive stress is successively greater than that at transition, relief, and harmless stresses. To a certain extent, when the stress-sensitivity coefficient increases, the permeability decreases much faster, and the stable period for production becomes shorter. For a reservoir with highly developed natural fractures, the stress-sensitivity coefficient is high, and the permeability damage mainly occurs in the stage when the reservoir pressure is less than the relief stress, and the depressurization rate could be 0.01–0.03 MPa/d. For reservoirs with fewer natural fractures, the opposite is the case, and the depressurization rate can be 0.05–0.07 MPa/d.

4) With an increase in the difference between the reservoir and desorption pressures, the effective stress at the desorption pressure increases and results in a relatively higher dynamic permeability damage; therefore, a significantly longer drainage time is required before desorption. A smaller difference between the reservoir and desorption pressures is more favorable for drainage and high gas production.

Acknowledgment This research was supported by National Science and Technology Major Project (No. 2017ZX05064) and the National Natural Science Foundation of China (Grant Nos. 42130806, 41830427, and 41922016).

Nomenclature

a is the fracture width, cm;

C is the stress sensitivity coefficient, MPa^{-1};

C_f is the stress sensitivity coefficient of fracture, MPa^{-1}

k is the permeability under different effective stresses, mD;

k' is the first-derivative of k.

k'' is the second-derivative of k;

k_f is the fracture permeability, mD;

k_0 is the initial permeability, mD, that is, the permeability when σ_e is 0 MPa;

k_{f0} is the original fracture permeability, mD;

k_D is the permeability damage rate;

K_q is the curvature of the stress-sensitive curve;

K'_q is the first-derivative of the curvature;

K''_q is the second-derivative of the curvature;

Φ_f is the fracture porosity;

σ_e is the effective stress, MPa;

σ_m is the sensitive stress, MPa;

σ_z is the transition stress, MPa.

References

Busse J, de Dreuzy J, Galindo Torres S, Bringemeier D, Scheuermann A (2017). Image processing based characterisation of coal cleat networks. Int J Coal Geol, 169(1): 1–21

Cai Y, Li Q, Liu D, Zhou Y, Lv D (2018). Insights into matrix compressibility of coals by mercury intrusion porosimetry and N_2 adsorption. Int J Coal Geol, 200(11): 199–212

Cai Y, Liu D, Mathews J P, Pan Z, Elsworth D, Yao Y, Li J, Guo X (2014). Permeability evolution in fractured coal-combining triaxial confinement with X-ray computed tomography, acoustic emission and ultrasonic techniques. Int J Coal Geol, 122: 91–104

Chen D, Pan Z, Liu J, Connell L (2012). Characteristic of anisotropic coal permeability and its impact on optimal design of multi-lateral well for coalbed methane production. J Petrol Sci Eng, 88–89(6): 13–28

Chen D, Pan Z, Liu J, Connell L (2013). An improved relative permeability model for coal reservoirs. Int J Coal Geol, 109–110: 45–57

Chen S, Qin Y, Shen J, Wang G, Hou X (2014). Temperature-stress sensitivity of high-rank coal permeability. J China Coal Soc, 39(9): 1845–1851 (in Chinese)

Cheng X, Luan H, Chen L, Jiang Y, Han W (2021). Numerical investigation on mechanical properties of in homogeneous coal under uniaxial compression and the role of cleat distribution. Bull Eng Geol Environ, 80(9): 7009–7027

Clarkson C, Qanbari F (2016). A semi-analytical method for forecasting wells completed in low permeability, undersaturated CBM reservoirs. J Nat Gas Sci Eng, 30(3): 19–27

Fan L, Liu S (2019). Evaluation of permeability damage for stressed coal with cyclic loading: an experimental study. Int J Coal Geol, 216(9): 103338

Feng Q, Jia H, Huang Z, Tian M, Li J, Li X (2018). Calculation model for water influx and controlled reserves for CBM wells with high water yield. Petrol Res, 3(3): 288–292

Feng R, Chen S, Bryant S (2019). Investigation of anisotropic deformation and stress-dependent directional permeability of coalbed methane reservoirs. Rock Mech Rock Eng, 53(8): 625–639

Fu X, Dai J, Feng J (2018). Prediction of tectonic fractures in coal reservoirs using geomechanical method. Geosci J, 22(4): 589–608

Geng Y, Tang D, Xu H, Tao S, Tang S, Ma L, Zhu X (2017). Experimental study on permeability stress sensitivity of reconstituted granular coal with different lithotypes. Fuel, 202(8): 12–22

Guo P, Cheng Y, Jin K, Li W, Tu Q, Liu H (2014). Impact of effective stress and matrix deformation on the coal fracture permeability. Transp Porous Media, 103(1): 99–115

Han G, Ling K, Zhang H (2016). Smart de-watering and production system through real-time water level surveillance for coal-bed methane wells. J Nat Gas Sci Eng, 31(4): 769–778

Hou D, Zhang H, Li G (2015). Study of pressure propagation characteristics to determine stress sensitivity of low-permeability gas reservoir. Chem Technol Fuels Oils, 51(2): 181–189

Huang Q, Fu X, Zhang Q, Li Y (2019). Experimental study on overburden pore permeability of medium and high rank coal reservoirs in Qinshui Basin. Coal Sci Techn, 47(6): 164–170 (in Chinese)

Jasinge D, Ranjith P, Choi S (2011). Effects of effective stress changes on permeability of latrobe valley brown coal. Fuel, 90(3): 1292–1300

Jia H, Sun S, Mao C, Wu Z, Lou T, Lou D (2017). Study on single-phase flow water production law of coalbed methane well based on coal and rock stress sensitivity. Coal Sci Techn, 45(12): 189–193 (in Chinese)

Kong X, Wang E, Liu Q, Li Z, Li D, Cao Z, Niu Y (2017). Dynamic permeability and porosity evolution of coal seam rich in CBM based on the flow-solid coupling theory. J Nat Gas Sci Eng, 40(4): 61–71

Li B, Wei J, Wang K, Li P, Wang K (2014a). A method of determining the permeability coefficient of coal seam based on the permeability of loaded coal. Int J Min Sci Technol, 24(5): 637–641

Li B, Zhu W, Liu Y, Ma Q, Zhang L, Yue M (2021). Experimental study and production model of multiscale stress sensitivity in tight oil reservoirs. Energy Sources A Recovery Util Environ Effects: 1–12

Li S, Tang D, Pan Z, Xu H, Huang W (2013). Characterization of the stress sensitivity of pores for different rank coals by nuclear magnetic resonance. Fuel, 111(9): 746–754

Li X, Fu X, Ranjith P, Xu J (2019). Stress sensitivity of medium- and high volatile bituminous coal: an experimental study based on nuclear magnetic resonance and permeability-porosity tests. J Petrol Sci Eng, 172(2): 889–910

Li Y, Tang D, Xu H, Meng Y J, Li J (2014b). Experimental research on coal permeability: the roles of effective stress and gas slippage. J Nat Gas Sci Eng, 21(11): 481–488

Li Y, Yang J, Pan Z, Tong W (2020). Nanoscale pore structure and mechanical property analysis of coal: an insight combining AFM and SEM images. Fuel, 260(1): 116352

Li Y, Zhang C, Tang D, Gan Q, Niu X, Wang K, Shen R (2017). Coal pore size distributions controlled by the coalification process: an

experimental study of coals from the Junggar, Ordos and Qinshui basins in China. Fuel, 206(10): 352–363

Lin Y, Qin Y, Ma D, Zhao J (2020). Experimental research on dynamic variation of permeability and porosity of low-rank inert-rich coal under stresses. ACS Omega, 5(43): 28124–28135

Liu D, Zou Z, Cai Y, Qiu Y, Zhou Y, He S (2021). An updated study on CH_4 isothermal adsorption and isosteric adsorption heat behaviors of variable rank coals. J Nat Gas Sci Eng, 89: 103899

Liu H, Sang S, Xue J, Lan T, Xu H, Ren B, Liu S (2018b). Evolution and geochemical characteristics of gas phase fluid and its response to inter-well interference during multi-well drainage of coalbed methane. J Petrol Sci Eng, 162(3): 491–501

Liu Q, Wang J, Liu J, Yang Q, Huang W, Liu Y, Wang L (2022). Determining diffusion coefficients of coal particles by solving the inverse problem based on the data of methane desorption measurements. Fuel, 308(1): 122045

Liu Y, Li M, Yin G, Zhang D, Deng B (2018a). Permeability evolution of anthracite coal considering true triaxial stress conditions and structural anisotropy. J Nat Gas Sci Eng, 52(4): 492–506

Liu Z, Liu D, Cai Y, Yao Y, Pan Z, Zhou Y (2020). Application of nuclear magnetic resonance (NMR) in coalbed methane and shale reservoirs: a review. Int J Coal Geol, 218: 103261

McKee C, Bumb A, Koenig R (1988). Stress-dependent permeability and porosity of coal and other geologica formation. SPE Form Eval, 3(1): 81–91

Meng Y, Li Z, Lai F (2015). Experimental study on porosity and permeability of anthracite coal under different stresses. J Petrol Sci Eng, 133(9): 810–817

Meng Y, Tang D, Xu H, Qu Y, Li Y, Zhang W (2014). Division of coalbed methane desorption stages and its significance. Pet Explor Dev, 41(5): 612–617

Meng Z P, Li G Q (2013). Experimental research on the permeability of high-rank coal under a varying stress and its influencing factors. Eng Geol, 162(7): 108–117

Ni X, Tan X, Wang B, Fu X (2021). An evaluation method for types of low-production coalbed methane reservoirs and its application. Energy Rep, 7(11): 5305–5315

Omotilewa O, Panja P, Vega-Ortiz C, McLennan J (2021). Evaluation of enhanced coalbed methane recovery and carbon dioxide sequestration potential in high volatile bituminous coal. J Nat Gas Sci Eng, 91(7): 103979

Palmer I, Mansoori J (1998). How permeability depends on stress and pore pressure in coalbeds: a new model. SPE Reservoir Eval Eng, 1(6): 539–544

Reiss L (1980). The Reservoir Engineering Aspects of Fractured Formations. Houston: Gulf Publishing Company Book Division

Seidle J, Jeansonne M, Erickson D (1992). Application of matchstick geometry to stress dependent permeability in coals. In: SPE rocky mountain regional meeting. Casper: Society of Petroleum Engineers: 433–438

Shi J, Wu J, Zhang T, Sun Z, Jia Y, Fang Y, Li X (2019). Novel coalbed methane reservoir permeability and reserve evaluation method based on flowing material balance equation at dewatering stage. In: Proceedings of unconventional resources technology conference. Brisbane: URTeC: 1–16

St. George J D, Barakat M A (2001). The change in effective stress associated with shrinkage from gas desorption in coal. Int J Coal Geol, 45(2): 105–113

Su X, Feng Y, Chen J, Pan J (2001). The characteristics and origins of cleat in coal from western north China. Int J Coal Geol, 47(1): 51–62

Su X, Wang Q, Lin H, Song J, Guo H (2018). A combined stimulation technology for coalbed methane wells: part 1 theory and technology. Fuel, 233(12): 592–603

Sun F, Wang B, Li M, Liang H (2014). Major geological factors controlling the enrichment and high yield of coalbed methane in the southern Qinshui Basin. Acta Petrol Sin, 35(6): 1070–1079 (in Chinese)

Sun Z, Wu K, Shi J, Li Y, Jin T, Li Q, Li X (2019). Novel prediction methods for under-saturated coalbed methane wells: effect of drainage schedules. J Petrol Sci Eng, 181(10): 106215

Tang J, Zhu J, Shao T, Wang J, Jiang Y (2021). A coal permeability model with variable fracture compressibility considering triaxial strain condition. Nat Resour Res, 30(2): 1577–1595

Tao S, Wang Y, Tang D, Xu H, Lv Y, He W, Li Y (2012). Dynamic variation effects of coal permeability during the coalbed methane development process in the Qinshui Basin, China. Int J Coal Geol, 93(1): 16–22

Wang C, Zhang J, Chen J, Zhong R, Cui G, Jiang Y, Liu W, Chen Z (2021). Understanding competing effect between sorption swelling and mechanical compression on coal matrix deformation and its permeability. Int J Rock Mech Min Sci, 138(2): 104639

Wang D, Lv R, Wei J, Fu Q, Wang Y, Zhang P, Yu C, Yao B (2019). An experimental study of seepage properties of gas-saturated coal under different loading conditions. Energy Sci Eng, 7(3): 799–808

Xiao K, Zhang Z, Zhang R, Gao M, Xie J, Zhang A, Liu Y (2021). Anisotropy of the effective porosity and stress sensitivity of coal permeability considering natural fractures. Energy Rep, 7(11): 3898–3910

Xu B, Li X, Ren W, Chen D, Chen L, Bai Y (2017). Dewatering rate optimization for coal-bed methane well based on the characteristics of pressure propagation. Fuel, 188(1): 11–18

Yan Z, Wang K, Zang J, Wang C, Liu A (2019). Anisotropic coal permeability and its stress sensitivity. Int J Min Sci Technol, 29(3): 507–511

Zhang C, Zhang N, Pan D, Qian D, An Y, Yuan Y, Xiang Z, Wang Y (2018). Experimental study on sensitivity of porosity to pressure and particle size in loose coal media. Enegies, 11(9): 2274–2293

Zhang G, Ranjith P, Liang W, Haque A, Perera M, Li D (2019a). Stress-dependent fracture porosity and permeability of fractured coal: an *in-situ* X-ray tomography study. Int J Coal Geol, 213(9): 103279

Zhang J, Wei C, Ju W, Yan G, Lu G, Hou X, Zheng K (2019b). Stress sensitivity characterization and heterogeneous variation of the pore fracture system in middle-high rank coals reservoir based on NMR experiments. Fuel, 238: 331–344

Zhang X, Wu C, Wang Z (2019c). Experimental study of the effective stress coefficient for coal permeability with different water saturations. J Petrol Sci Eng, 182(9): 106282

Zhang Y, He Y, Yang Z, Liu X (2010). Experimental research on stress

sensitivity of coalbed reservoir. Natural Gas Geoscience, 21(3): 518–521 (in Chinese)

Zhang Z, Zhang R, Wu S, Deng J, Zhang Z, Xie J (2019d). The stress sensitivity and porosity sensitivity of coal permeability at different depths: a case study in the Pingdingshan mining area. Rock Mech Rock Eng, 52(5): 1539–1563

Zhang Z, Zhang R, Xie H, Gao M (2015). The relationships among stress, effective porosity and permeability of coal considering the distribution of natural fractures: theoretical and experimental analyses. Environ Earth Sci, 73(10): 5997–6007

Zhao Y, Wang Z, Xin X (2018). Experiment and model research on the influence of effective stress on the coal permeability. Mining Res Develop, 38(6): 54–60 (in Chinese)

Zhou D, Li K, Wang H, Jin Y, Ru Z, Xu X, Wu C, Jian K (2020). Permeability experiments with overburden pressure of coal measure reservoirs and numerical analysis of its stress sensitivity: a case study of Qinshui Basin, China. Energy Explor Exploit, 38(5): 1690–1705

Zhu H, Tang X, Liu Q, Liu S, Zhang B, Jiang S, McLennan J D (2018). Permeability stress-sensitivity in 4D flow-geomechanical coupling of Shouyang CBM reservoir, Qinshui Basin, China. Fuel, 232(11): 817–832

Zou C, Xue H, Xiong B, Zhang G, Pan S, Jia C, Wang Y, Ma F, Sun Q, Guan C, Lin M (2021). Connotation, innovation and vision of “carbon neutrality”. Nat Gas Indust B, 8(5): 523–537